Polish J. Chem., **78**, 35–43 (2004)

Carbonate-Containing Barium Hydroxyapatite Synthesized by Solid State Reactions

by E. Getman[1*], S. Loboda[1], A. Ignatov[1] and P. Demchenko[2]

[1]*Department of Inorganic Chemistry, Donetsk National University, Universitetskaya str., 24, 83055 Donetsk, Ukraine*
[2]*Department of Inorganic Chemistry, Lviv National University, Kyryla i Mefodiya str., 6, 79005 Lviv, Ukraine*

(Received June 23rd, 2003; revised manuscript August 14th, 2003)

The carbonate-containing barium hydroxyapatite was prepared by solid state reactions in air at 950°C. Obtained samples were investigated by X-ray powder diffraction and IR spectroscopy. The stoichiometry of these samples conforms to $Ba_5(PO_4)_{3-x}(CO_3)_x(OH)_{1-x}O_x$ as the result of CO_3^{2-} and O^{2-} substitution for PO_4^{3-} and OH^- in the hydroxyapatite lattice under the scheme: $PO_4^{3-} + OH^- \rightarrow CO_3^{2-} + O^{2-}$. The crystal structure of some carbonated barium hydroxyapatite patterns were refined by Rietveld method using X-ray powder diffraction data. The analysis of the crystallographic site occupation has shown that the single phase range of $Ba_5(PO_4)_{3-x}(CO_3)_x(OH)_{1-x}O_x$ is limited by $x = 0.32$.

Key words: hydroxyapatite, solid solution, barium

In recent years, the interest of researchers to compounds with the structure of apatite, and hydroxyapatites among them, has increased due to their application as artificial biomaterials compatible with a bone tissue, luminophor materials, sensor controls of moisture and alcohols, adsorbents of ecologically harmful and radioactive substances (Pb, Cd, F, U, Sr), catalysts of alcohols dehydration reactions, hydrolysis of chlorbenzene, conversion of methane and other cases [1–6]. In many respects such wide spectrum of applications is caused by ability of apatite to isomorphous substitution of other ions for Ca, P and OH group [7]. In particular, the incorporation of CO_3^{2-} into its structure has considerable influence on the physical and physico-chemical properties, as well as on the mineralization and demineralization processes [8,9]. Besides, in air there is always CO_2 and it exists the probability of spontaneous incorporation of CO_3^{2-} ions into the structure of apatite for the sites of OH^- groups (so-called A-type carbonated apatites) and PO_4^{3-} groups (so-called B-type carbonated apatites). Previously, the substitutions in the structure of calcium hydroxyapatite were mainly investigated. Therefore, the purpose of our study was the investigation of the substitution of CO_3^{2-} ion for PO_4^{3-} ion in the structure of barium hydroxyapatite, assuming the following scheme: $PO_4^{3-} + OH^- \rightarrow CO_3^{2-} + O^{2-}$ that corresponds to the $Ba_5(PO_4)_{3-x}(CO_3)_xO_x$ formula.

* Author for correspondence. E-mail: getman@dongu.donetsk.ua

EXPERIMENTAL

Preparation of samples. The mixtures of $BaCO_3$ and $(NH_4)_2HPO_4$ were composed so, that the molar ratio Ba/P conform to 5/(3-x) with $0 \leq x \leq 1$. Each mixture was homogenized in an agate mortar for 20 min and was heated in an alumina crucible at 300 and 800°C for 3 hours at each temperature. Then the samples were homogenized, pressed into tablets and heated in an electric furnace at 950°C. After sintering the products were quenched in air, powdered, and analyzed by X-ray powder diffraction. After that, the samples were pressed into tablets again and sintered at 950°C, until a constant phase composition was obtained. Total time of sintering at 950°C was 10 hours.

Physical analysis. X-ray powder diffraction patterns of the samples were recorded at room temperature, using a powder diffractometer DRON-2 with the Ni-filtered copper Kα radiation. The *a* and *c* parameters of the hexagonal unit cell of barium hydroxyapatite were calculated from the positions of 14 most intense and sharp reflections by using a least-squares refinement program. The scanning rate was 1°/min, Si was used as an external standard.

The measurements for crystal structure refinement were carried out in a step regime: step 0.05° 2θ, interval $15.00 \leq 2\theta \leq 140.00$, scanning rate 10 s per step. The profile analysis of X-ray powder diffraction data was performed using the method of approximation of X-ray reflections by pseudo-Voigt profile function. The lattice parameters and crystal structure of the phases were refined using Rietveld method with the program FULLPROF.2k (version 2.20) [10] from the WinPLOTR software [11].

IR spectra of the samples dispersed in KBr tablets were recorded using a Perkin-Elmer Fourier transform infrared spectrophotometer in the range 400–4000 cm^{-1}.

RESULTS AND DISCUSSION

In the $Ba_5(PO_4)_{3-x}(CO_3)_x(OH)_{1-x}O_x$ system the single-phase material with the apatite structure exists in the concentration range of $x = 0$–0.4. At larger *x* value, there are phases of hydroxyapatite and barium carbonate $BaCO_3$. Amounts of the latter phase increases with rising the *x* value.

The unit cell dimensions of the CO_3^{2-} – containing solid solution based on barium hydroxyapatite are presented in Figure 1. It is seen that when the *x* increases from 0 to 0.4, the *a* lattice parameter of the hexagonal unit cell of hydroxyapatite decreases and *c* parameter increases concurrently. The parameters became practically constant as *x* increases further. Such changes in the unit cell dimensions of the CO_3^{2-} – containing barium hydroxyapatite, indicate that the limit of a single-phase range equals $x \approx 0.4$. This value is also obtained by the method of "disappearing phase" [12]. The straight line of the *x*-dependence of the 111 reflection intensity cuts the abscissa axis at $x \approx 0.4$. This is illustrated in Figure 2.

The crystal structure refinement was performed on the samples $Ba_5(PO_4)_{3-x}(CO_3)_x(OH)_{1-x}O_x$ at compositions $x = 0.0$, $x = 0.2$ and $x = 0.4$. The allocations of corresponding atoms by the crystallographic sites and their coordinates in the calcium hydroxyapatite structure, represented in [9], were used as starting data for the calculations. The statistical distribution of the P and C atoms, O-atoms and OH-group over the 6*h* and 4*e* sites was assumed. Crystallographic and experimental data are given in Table 1, atomic parameters – in Table 2. Comparison of experimental and calculated powder patterns is presented on Fig. 3. According to the X-ray phase analysis, samples of compositions $x = 0.0$ and $x = 0.2$ were single-phase samples,

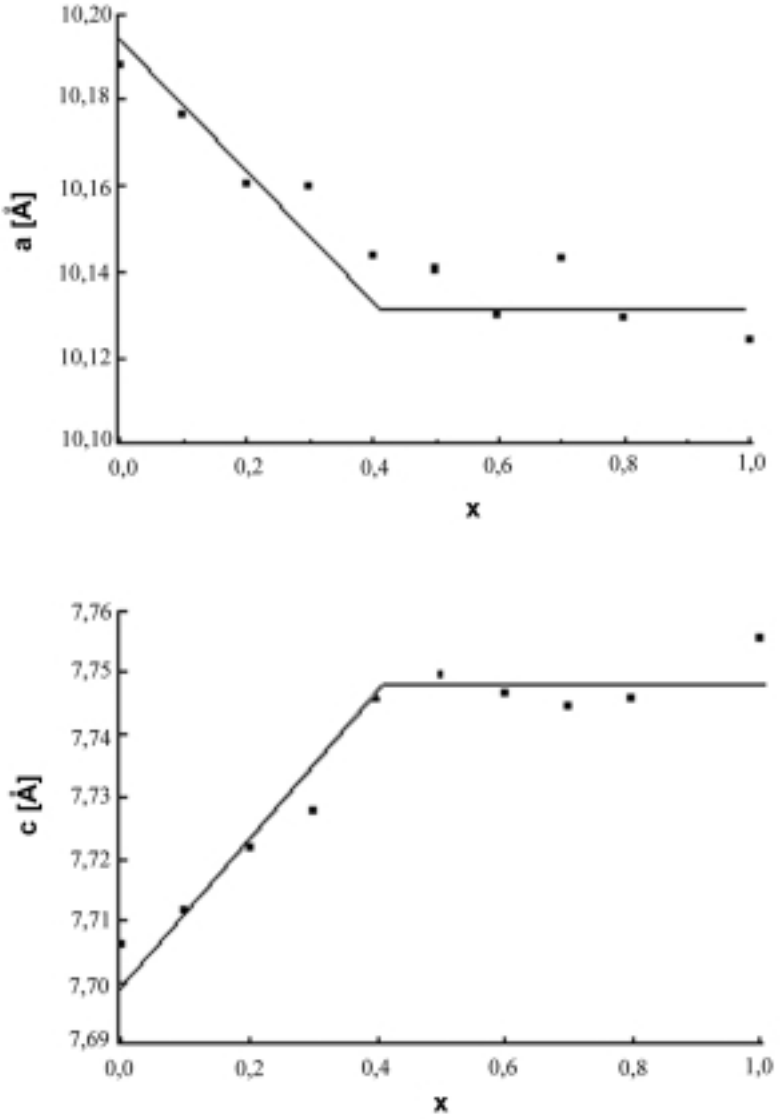

Figure 1. Dependence of the $Ba_5(PO_4)_{3-x}(CO_3)_x(OH)_{1-x}O_x$ hexagonal unit cell dimensions *versus* composition.

while the sample at $x = 0.4$ contained a small amount of the $BaCO_3$. The initial refinement was performed using two-phase model. The results of refinement showed, that the content of additional phase, determined by Rietveld method, is small (~3%); in spite of this the single-phase model was used in following calculations. The analysis of the occupation factors G has shown that the limited composition of monophase $Ba_5(PO_4)_{3-x}(CO_3)_x(OH)_{1-x}O_x$ is situated at $x = 0.32$.

Table 1. Crystallographic and experimental data for the $Ba_5(PO_4)_{3-x}(CO_3)_x(OH)_{1-x}O_x$ – phases.

Phase	$Ba_5(PO_4)_{3-x}(CO_3)_x(OH)_{1-x}O_x$		
	x = 0	x = 0.2	x = 0.4
Space group	——	$P6_3/m$	——
Structure type	——	Apatite	——
Lattice parameters (nm)			
a	1.01964(2)	1.01604(3)	1.01520(4)
c	0.77111(2)	0.77316(3)	0.77531(3)
Cell volume (nm^3)	0.69428(3)	0.69123(4)	0.69200(5)
Radiation and wavelengths (Å)	——	Cu Kα 1.54056 1.54439	——
Mode of refinement		Full profile	
Angular range $2\theta_{min}$–$2\theta_{max}$ (degrees)		15.00–140.00	
Number of measured reflections	976	968	978
Reliability factors:			
$R_B=\Sigma\|I_h(obs)-I_h(calc)\| / \Sigma\|I_h(obs)\|$	0.0518	0.0662	0.0690
$R_F=\Sigma\|\|F_h(obs)\|-\|F_h(calc)\|\| / \Sigma\|F_h(obs)\|$	0.0513	0.0536	0.0514
$R_p=\Sigma\|y_i(obs)-y_i(calc)\| / \Sigma y_i(obs)$	0.0968	0.0963	0.0767
$R_{wp}=[\Sigma w_i\|y_i(obs)-y_i(calc)\|^2 / \Sigma w_i y_i(obs)^2]^{1/2}$	0.136	0.128	0.0990
$\chi^2=\{R_{wp}/R_{exp}\}^2$	1.58	1.39	1.80

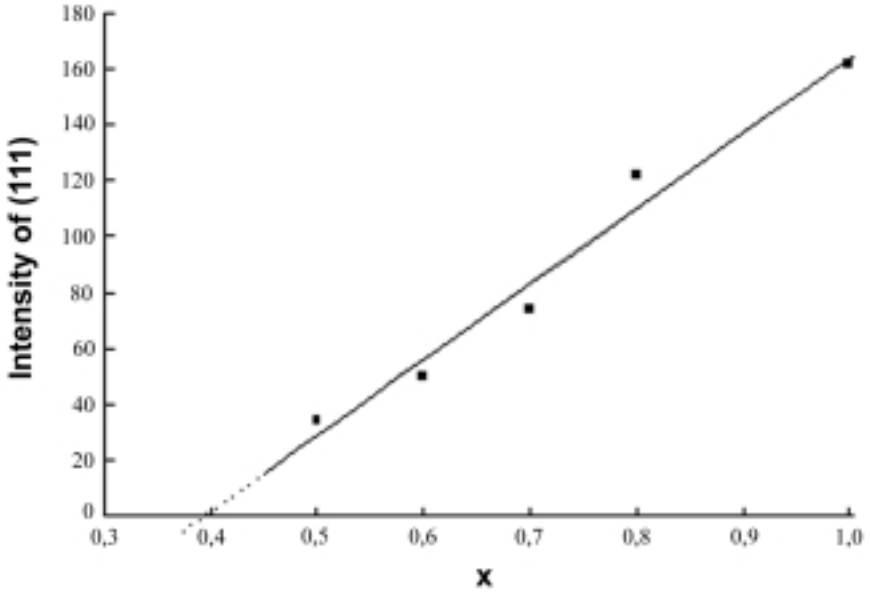

Figure 2. Dependence of the intensity of the barium carbonate 111 reflection *versus* composition.

Table 2. Atomic parameters, displacements (B_{iso}) and occupations (G) for the $Ba_5(PO_4)_{3-x}(CO_3)_x(OH)_{1-x}O_x$ – phases.

Atom	Site	Parameter	$Ba_5(PO_4)_{3-x}(CO_3)_x(OH)_{1-x}O_x$		
			x = 0	x = 0.2	x = 0.4[a]
Ba1	4*f*	*x*	2/3	2/3	2/3
		y	1/3	1/3	1/3
		z	–0.0005(7)	0.0009(7)	0.0008(6)
		B_{iso}, Å^2	0.89(5)	0.73(6)	0.63(5)
		G	1	1	1
Ba2	6*h*	*x*	0.2426(3)	0.2379(3)	0.2381(3)
		y	0.9819(3)	0.9818(4)	0.9823(3)
		z	1/4	1/4	1/4
		B_{iso}, Å^2	0.95(5)	1.38(6)	1.59(6)
		G	1	1	1
P	6*h*	*x*	0.403(1)	0.409(1)	0.408(1)
		y	0.372(1)	0.374(1)	0.376(1)
		z	1/4	1/4	1/4
		B_{iso}, Å^2	1.0(2)	0.7(3)	0.5(2)
		G	1	0.933	0.89(2)
C	6*h*	*x*	–	0.409(1)	0.408(1)
		y		0.374(1)	0.376(1)
		z		1/4	1/4
		B_{iso}, Å^2		0.7(3)	0.5(2)
		G		0.067	0.11(2)
O1	6*h*	*x*	0.340(3)	0.345(3)	0.341(3)
		y	0.479(3)	0.485(3)	0.480(2)
		z	1/4	1/4	1/4
		B_{iso}, Å^2	1.3(6)	1.9(7)	0.7(6)
		G	1	1	1
O2	6*h*	*x*	0.578(3)	0.577(3)	0.583(3)
		y	0.456(3)	0.460(3)	0.467(3)
		z	1/4	1/4	1/4
		B_{iso}, Å^2	0.9(6)	2.8(8)	2.0[b]
		G	1	1	1
O3	12*i*	*x*	0.354(2)	0.353(2)	0.357(2)
		y	0.271(2)	0.271(2)	0.273(2)
		z	0.081(2)	0.082(2)	0.084(2)
		B_{iso}, Å^2	2.0(5)	2.3(5)	1.3(4)
		G	1	0.983	0.95(2)
OH	4*e*	*x*	0	0	0
		y	0	0	0
		z	0.147(5)	0.112(6)	0.085(4)
		B_{iso}, Å^2	5(1)	7(1)	4(1)
		G	0.5	0.4	0.34(3)
O4	4*e*	*x*	–	0	0
		y		0	0
		z		0.112(6)	0.085(4)
		B_{iso}, Å^2		7(1)	4(1)
		G		0.1	0.16(3)

[a] – Sample contained small amount (~3%) of additional phase $BaCO_3$;
[b] – fixed value.

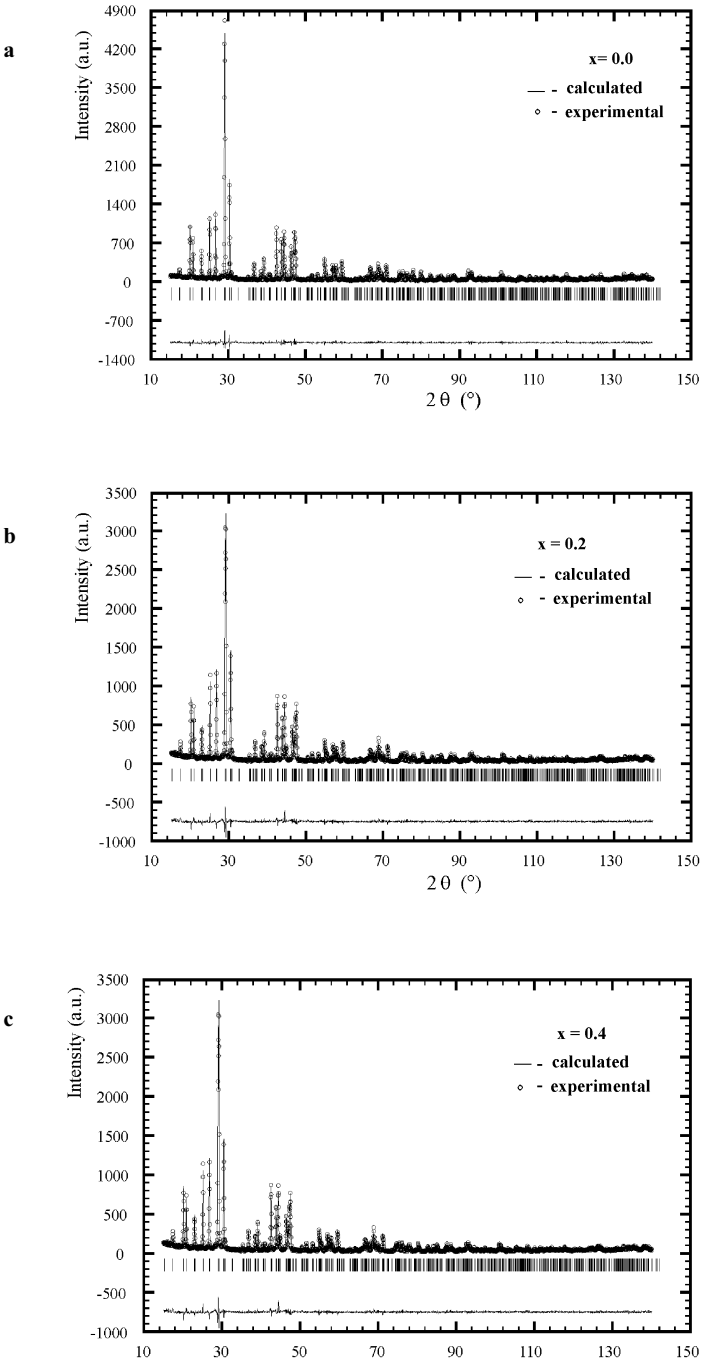

Figure 3. Observed (circles), calculated (solid line) and differential (bottom) X-ray powder profiles (Cu *Kα*-radiation) for $Ba_5(PO_4)_{3-x}(CO_3)_x(OH)_{1-x}O_x$ – phases: (a) – x = 0.0, (b) – x = 0.2, (c) – x = 0.4.

IR spectra of CO_3^{2-} – containing barium hydroxyapatite, are represented in Figure 4. Unsubstituted barium hydroxyapatite $Ba_5(PO_4)_3OH$ displays typical absorptions, arising from PO_4^{3-} (933 – ν_1, 443 – ν_2, 1013 and 1054 – ν_3, 556 and 581 cm^{-1} – ν_4), absorbed water (broad peak in the range 3200–3650 cm^{-1} arising from OH^- connected by hydrogen bonds and 1630 cm^{-1}), hydroxyl group which are not included in water (430 cm^{-1} – librational mode) [13,14]. In the spectra of the samples of substituted hydroxyapatite the positions and intensities of absorptions, arising from PO_4^{3-} and from absorbed water, are the same. There is only a spurious reduction of the absorption at 933 cm^{-1}, which is probably caused by expansion of the absorption at 1013 cm^{-1}. Increase of the "x" value is accompanied by some decrease of the absorption bands of OH^- at 430 cm^{-1} and absorbed water (broad peak 3200–3600 and 1630 cm^{-1}). Absorptions at 867, 1390, 1425 and 1460 cm^{-1} caused by the vibrations of CO_3^{2-} located on the PO_4^{3-} lattice site (B-type carbonated apatite) are also observed. The absorptions bands of CO_3^{2-} show a rise with increase of the *x* value. It is necessary to note, that in the spectrum of unsubstituted barium hydroxyapatite (x = 0) there are the bands attributed to CO_3^{2-} ion, located on the PO_4^{3-} lattice site with an intensity greater than in the spectrum of unsubstituted strontium hydroxyapatite.

In addition, in the spectra of barium hydroxyapatites the band attributed to the vibration of CO_3^{2-} located on the OH^- lattice site (A-type carbonated apatite) at 1537 cm^{-1} [15], was not observed.

The methods of synthesis of B-type carbonated apatites have been known previously. Decrease of the negative charge, caused by CO_3^{2-} for PO_4^{3-} substitution in the anionic sublattice, was compensated by two means. In the first case, the corresponding amount of alkaline metal cations instead of bivalent metal cations

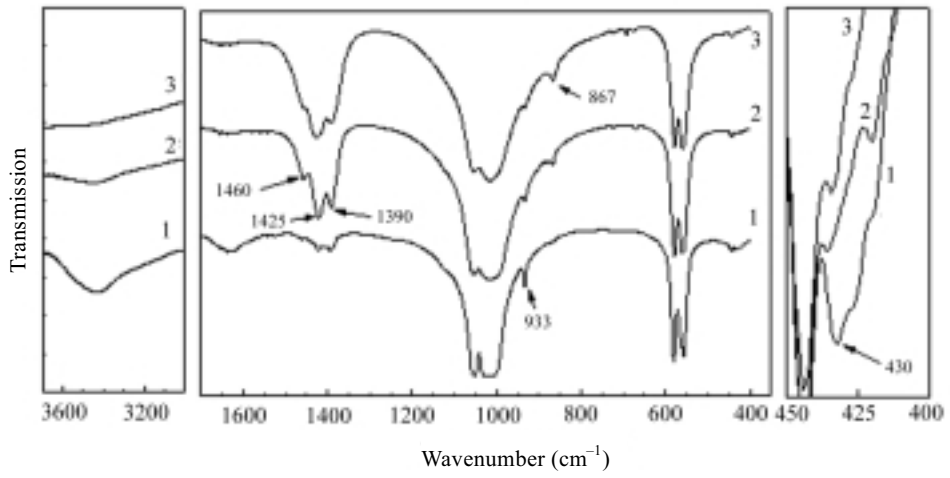

Figure 4. IR spectra of the $Ba_5(PO_4)_{3-x}(CO_3)_x(OH)_{1-x}O_x$ samples in the range 400–450 cm^{-1}, 400–1800 cm^{-1} and 3000–3700 cm^{-1} [1) x = 0; 2) x = 0.2; 3) x = 0.4].

was incorporated in the structure of apatite. So sodium containing B-type carbonated hydroxyapatite has been obtained by hydrolysis of monetite (substitution $Ca^{2+} + PO_4^{3-} \rightarrow Na^+ + CO_3^{2-}$ and $Ca^{2+} + PO_4^{3-} + OH^- \rightarrow V_{Ca} + CO_3^{2-} + V_{OH}$ has been realized). Potassium containing carbonated hydroxyapatite with composition of $Ca_{10-x}K_x[(PO_4)_{6-x}(CO_3)_x][(OH)_{2-y}(CO_3)_y]$ (substitution under the schemes: $Ca^{2+} + PO_4^{3-} \rightarrow K^+ + CO_3^{2-}$ and $2OH^- \rightarrow CO_3^{2-} + V_{OH}$) has been obtained by solid state reactions in dry CO_2 atmosphere. Actually, those were mixed A- and B-type carbonated hydroxyapatites [8]. Potassium containing apatite as the result of ions substitution under the schemes: $Ca^{2+} + PO_4^{3-} \rightarrow K^+ + CO_3^{2-}$ and $Ca^{2+} + PO_4^{3-} + OH^- \rightarrow V_{Ca} + CO_3^{2-} + V_{OH}$ has been obtained by hydrolysis of octacalcium phosphate [9].

In the second case the carbonated hydroxyapatite, which does not contain an alkaline metal cation, has been obtained by precipitation from aqueous solutions. However, its composition differs from the "classical" hydroxyapatite in lesser amount of earth metal cations: $Ca_9(PO_4)_4(CO_3OH)_2$, $Ca_{10-x}(PO_4)_{6-2x}(CO_3A)_{2x}A_{2(1-x)}$, where $A - OH^-, F^-$ [15], $Ca_{10-x+u}(PO_4)_{6-x}(CO_3)_x(OH)_{2-x+2u}$ [16]. Thus, the substitution of CO_3^{2-} ion for PO_4^{3-} ion occurs under the following schemes:

$Me^{2+} + PO_4^{3-} + OH^- \Leftrightarrow V_{Me} + CO_3^{2-} + V_{OH}$ (I), $Me^{2+} + 2PO_4^{3-} \Leftrightarrow V_{Me} + 2CO_3^{2-}$ (II), $Me^{2+} + PO_4^{3-} \Leftrightarrow Me^+ + CO_3^{2-}$ (III), $2OH^- \Leftrightarrow CO_3^{2-} + V_{OH}$ (IV), $PO_4^{3-} \Leftrightarrow (CO_3OH)^{3-}$ (V).

The possibility of the substitution, according to the $PO_4^{3-} + OH^- \rightarrow CO_3^{2-} + O^{2-}$ scheme, has not been considered in the afore-mentioned articles. According to our data, such substitution takes place in barium hydroxyapatites, and B-type carbonated hydroxyapatite is formed as the result. The evidences of this statement are: 1. Materials formed in an interval of $x = 0–0.4$ are single-phase solid solutions. Impurity phases would appear in the case of an other substitution scheme. 2. The variations of the unit cell dimensions of barium hydroxyapatites with the dopant concentration are the same, as those of previously described B-type carbonated hydroxyapatite: *a* decreases and *c* increases with increasing the *x* value. 3. In the IR spectra the bands typical for B-type carbonated hydroxyapatite are observed in the range 1400–1460 cm^{-1} and the bands typical for A-type carbonated hydroxyapatite are absent in the range 1530–1540 cm^{-1}. 4. According to XRD data, CO_3^{2-} and PO_4^{3-} ions are statistically distributed over the lattice site.

REFERENCES

1. Inorganic Phosphate Materials, Ed. T. Kanazawa, Amsterdam 1989, p. 298.
2. Sugiyama S., Abe K., Minami T., Hayashi H. and Moffat J.B., *Applied Catalysis A: General*, **169**, 77 (1998).
3. Sugiyama S., Minami T., Higaki T., Hayashi H. and Moffat J.B., *Ind. Eng. Chem. Res.*, **36**, 328 (1997).
4. Ramesh R. and Jagannathan R., *J. Phys. Chem. B.*, **104**, 8351 (2000).
5. Arey J.S., Seaman J.C. and Bertsch P.M., *Envi. Sci. Techn.*, **33**, 337 (1999).
6. Chen X., Wright J.V., Conca J.V. and Peurrung L.M., *Env. Sci & Techn.*, **31**, 624 (1997).
7. Mineralogical Encyclopaedia, Ed. K. Frey, Leningrad 1985, p. 512.
8. Verbeeck R.M.H., De Maeyer E.A.P. and Driessens F.C.M., *Inorg. Chem.*, **34**, 2084 (1995).

9. De Maeyer E.A.P., Verbeeck R.M.H. and Naessens D.E., *Inorg. Chem.*, **32**, 5709 (1993).
10. Rodriguez-Carvajal J., Program FullProf.2k (version 2.20 – September 2002 – LLB JRC) (unpublished).
11. Roisnel T. and Rodriguez-Carvajal J., "WinPLOTR: a Windows tool for powder diffraction patterns analysis", Materials Science Forum, Proceedings of the Seventh European Powder Diffraction Conference (EPDIC 7), Barcelona, 2000, pp. 118–123, Eds. R. Delhez and E.J. Mittenmeijer.
12. Kachanov N. and Mirkin L., X-ray structure analysis, Moscow 1960, p. 211.
13. Engel G. and Klee W.E., *J. Solid State Chem*., **5**, 28 (1972).
14. Klee W.E. and Engel G., *J. Inorg. Nucl. Chem.*, **32**, 1837 (1970).
15. Bonel G., *Ann. Chim.*, **7**, 65 (1972).
16. Labarthe J.-C. and Bonel G., *Ann. Chim*., **8**, 289 (1973).